

PROBING THE DARK AGES AT $Z \sim 20$: THE SCI-HI 21 CM ALL-SKY SPECTRUM EXPERIMENT

TABITHA C. VOYTEK^{1,*}, ARAVIND NATARAJAN^{1,2}, JOSÉ MIGUEL JÁUREGUI GARCÍA³, JEFFREY B. PETERSON¹, OMAR LÓPEZ-CRUZ³

Draft version May 22, 2022

ABSTRACT

We present first results from the SCI-HI experiment, which we used to measure the all-sky-averaged 21 cm brightness temperature in the redshift range $14.8 < z < 22.7$. The instrument consists of a single broadband sub-wavelength size antenna and a sampling system for real-time data processing and recording. Preliminary observations were completed in June 2013 at Isla Guadalupe, a Mexican biosphere reserve located in the Pacific Ocean. The data was cleaned to excise channels contaminated by radio frequency interference (RFI), and the system response was calibrated by comparing the measured brightness temperature to the Global Sky Model of the Galaxy. We present our results, discuss the cosmological implications, and describe plans for future work.

1. INTRODUCTION

Emission and absorption due to the 21 cm spin flip transition of neutral Hydrogen (HI) have emerged as valuable tools to probe the physics of the Universe at early times (Loeb & Zaldarriaga 2004; Cooray 2004; Bharadwaj & Ali 2004; Carilli et al. 2004; Furlanetto & Briggs 2004; Furlanetto et al. 2006; Pritchard & Loeb 2010, 2012; Liu et al. 2013). Experiments studying the early universe through the 21 cm transition are of two kinds: mapping experiments that measure the power spectrum of 21 cm fluctuations and all-sky absolute brightness experiments that measure the averaged 21 cm brightness temperature. Mapping experiments include PAPER (Pober et al. 2013; Parsons et al. 2013), GMRT-EoR (Paciga et al. 2011), LOFAR (van Haarlem et al. 2013), MWA (Bernardi et al. 2013), and the proposed Hydrogen Epoch of Reionization Array (HERA) (2010) and Square Kilometer Array (SKA) (2013). All-sky experiments include EDGES (Bowman et al. 2008) and the proposed Large-Aperture Experiment to detect the Dark Ages (LEDA) (2013) and Dark Ages Radio Explorer (DARE) (Burns et al. 2012).

The first stars to form are composed almost entirely of primordial elements. These stars, called Pop. III.1, are thought to form in dark matter minihalos of mass $\approx 10^6 - 10^8 M_\odot$ at a redshift $z \approx 20-30$ (Bromm et al. 1999, 2002; Bromm & Larson 2004; Abel et al. 2002; Omukai & Palla 2001, 2003; Tan & McKee 2004; McKee & Tan 2008; Bromm 2013), and provide UV illumination of the HI. Supernovae from these short lived, massive stars enriched the Universe with heavy elements, paving the way for the subsequent generation of lower mass stars and planets. Formation of the first stars is thus a sub-

ject of broad impact, but it is difficult to constrain these models due to the absence of observations at high redshifts. The observations presented here aim to provide such constraints.

Formation of the first stars results in the production of Lyman- α photons, which are efficient in coupling the spin (T_s) and kinetic (T_k) temperatures of HI through the Wouthuysen-Field mechanism (Wouthuysen 1952; Field 1958). At $z \approx 20-30$ the neutral gas kinetic temperature $T_k \propto (1+z)^2$ is well below the CMB temperature (T_γ). The Wouthuysen-Field mechanism sets $T_s = T_k$, and predicts a significant trough in the 21 cm brightness temperature (T_b) around the redshift of first star formation, with $T_b \propto (T_s - T_\gamma)/T_s \approx -T_\gamma/T_k$. Later, heating of the gas by high energy radiation sets $T_s = T_k \gg T_\gamma$. T_b then enters the emission saturation regime where it is small and positive, before decreasing to zero as the Universe reionizes. The magnitude and width of the trough in the 21 cm brightness temperature, provide valuable information on the properties of the first stars and X-ray sources. This trough is also the most easily measurable feature in the all-sky spectrum (Liu et al. 2013).

In the following sections we describe the experiment "Sonda Cosmológica de las Islas para la Detección de Hidrógeno Neutro" (SCI-HI). This experiment measures the 21 cm brightness temperature using a single antenna and attendant sampling system operating on-site in a radio quiet location. Calibrated, Galaxy-subtracted data collected June 1-15, 2013 is presented and cosmological implications are discussed.

2. EXPERIMENTAL SETUP

In order to probe the 21 cm all-sky structure, we designed a single antenna experiment that is optimized to work from 40-130 MHz, with over 90% antenna coupling efficiency from 55-90 MHz. The entire system is designed to run off 12V DC batteries, allowing the experiment to be portable and easy to set up in remote locations.

2.1. *Hibiscus Antenna*

Our antenna design started with the need to observe over an octave of frequency. Using FEKO, a finite element simulation, a four-square antenna scaled to 70 MHz

* tcv@andrew.cmu.edu

¹ McWilliams Center for Cosmology, Carnegie Mellon University, Department of Physics, 5000 Forbes Ave., Pittsburgh PA 15213, USA

² Department of Physics and Astronomy & Pittsburgh Particle physics, Astrophysics and Cosmology Center, University of Pittsburgh, 100 Allen Hall, 3941 O'Hara Street, Pittsburgh, PA 15260

³ Instituto Nacional de Astrofísica, Óptica y Electrónica (INAOE), Coordinación de Astrofísica, Luis Enrique Erro No. 1 Sta. Ma. Tonantzintla, Puebla, 72840 Mexico

was modified by dividing the square plates into inclined trapezoidal sections. The exact size, angles and spacing of the sections were tuned to increase performance and a 1:6 scale model was built with the best design. This model was tested in an antenna range to determine the real antenna bandwidth, impedance and beam shape and enable fine adjustments.

Critical parameters are the space between sections and the height above the ground plane. The first parameter changes the impedance and the second parameter impacts the beam pattern. The antenna is fixed and points to the zenith. Our final design has increased bandwidth, a flattened impedance curve and a 55° beam at 70 MHz with uniform shape. A more detailed description can be found in (Jáuregui-García et al in preparation) and the antenna is shown in Fig 1. We call this new design the Hibiscus antenna.

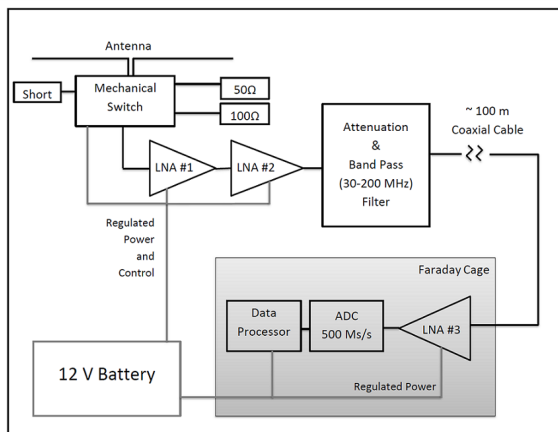


FIG. 1.— SCI-HI experiment. Top: Hibiscus Antenna on-site on Isla Guadalupe, Mexico. Bottom: System Block Diagram

2.2. Sampling system

A basic block diagram is shown in Fig. 1. The signal from our antenna passes through a series of electronic stages, including amplifiers and filters to remove radio frequency interference (RFI) below 30 MHz and aliasing from signals above 200 MHz. To measure the noise of the system, an electro-mechanical switch is placed between the antenna and the first amplifier. This switch, controlled by the sampling software, collects spectra from terminators of known temperature (50Ω , 100Ω and Short). These spectra are collected in 5 min intervals and are used for calibration, as is shown in Eqn. 2.

The sampling system is composed of a GE PCIe digitizer board (ICS1650) for data acquisition and a PC with software for power spectrum generation. Signal from the antenna is sampled at 500 MSamples/sec with 12 bits of resolution, after which Fourier transform routines integrated into the sampling software are used to generate power spectra from 0-250 MHz. The system is placed inside of a Faraday cage ~ 50 meters from the antenna and all power/control signals sent to the antenna and electronics as well as power to the internal PC buses are RF filtered to minimize self-generated noise contamination. To minimize data collection interruptions, an external supervisor circuit monitors the system to provide restart in case of failure. The data sampling/processing duty cycle is $\sim 10\%$, so 1 day of observation yields about 2 hours of effective observation time.

2.3. Experimental Sites

One major noise contribution in this frequency range is terrestrial RFI. In particular, television stations and FM radio stations transmit in our band. Even at the U.S. National Radio Quiet Zone in Green Bank, West Virginia, the FM signal exceeds the sky signal by 10 dB over the entire FM band of 88-108 MHz.

In order to bring RFI down below the level of the expected signal, it is necessary to operate the instrument at an extremely remote radio-quiet location. For the data presented here, we travelled to Isla Guadalupe in Mexico. Isla Guadalupe (Latitude $28^\circ 58' 24''$ N, Longitude $118^\circ 18' 4''$ W), is 260 km off the Baja California peninsula in the Pacific Ocean. It is a Mexican biosphere reserve and has minimal infrastructure. As the location is a biosphere reserve, we took extreme measures to ensure that our experiment had limited impact on the fragile insular ecosystem.

We spent two weeks on Isla Guadalupe (June 1-15, 2013) collecting data on the western side of the island. Even at this remote site, we still detect some RFI from the mainland, although residual FM is only about 0.1 dB (≤ 70 K) above the Galactic foreground level and there are no other strong RFI signals in our band.

3. RESULTS

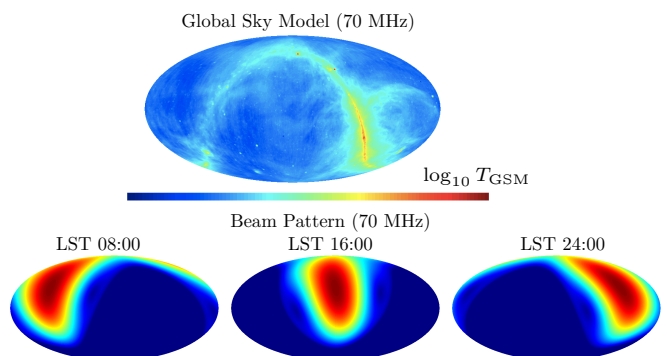


FIG. 2.— Sky temperature and antenna beam pattern in (RA, DEC) coordinates. The top row shows the sky temperature (logarithmic) at 70 MHz, from the Galactic Global Sky Model (GSM). The bottom row shows the simulated antenna beam pattern at 70 MHz at different LST, plotted for the latitude of Isla Guadalupe.

The Galactic Global Sky Model (GSM) (de Oliveira-Costa et al. 2008) provides a set of maps of the Galaxy

at frequencies between 10 MHz and 100 GHz, created by interpolating data derived from publicly available large area radio surveys. GSM software is used to produce a set of maps of the sky in the frequency range relevant to our observations. For each frequency, the beam-averaged sky temperature as a function of time may then be obtained:

$$T_{\text{GSM}}(t, \nu) = \frac{\int d\Omega \text{GSM}(\theta, \phi, \nu) \mathcal{B}(\theta - \theta_0(t), \phi - \phi_0(t), \nu)}{\int d\Omega \mathcal{B}(\theta - \theta_0(t), \phi - \phi_0(t), \nu)} \quad (1)$$

where (θ, ϕ) are (RA, DEC) co-ordinates, $\mathcal{B}(\theta, \phi, \nu)$ is the antenna beam pattern, and $(\theta_0(t), \phi_0(t))$ is the beam center. The time dependence of (θ_0, ϕ_0) arises due to the rotation of the earth. Fig. 2 shows the GSM map at 70 MHz (top row) as well as the antenna beam pattern for 3 different values of Local Sidereal Time (LST). The sky brightness is greatest when the beam center crosses the Galactic plane, and smallest when the Galactic plane aligns with the horizon.

The spectra from our observations are cleaned to excise RFI contaminated data and calibrated by defining:

$$T_{\text{meas}}(t, \nu) = K(\nu) \left[\frac{P_{\text{meas}}(t, \nu)}{\eta(\nu)} - P_{\text{short}}(\nu) \right] \quad (2)$$

Where $K(\nu)$ is the system gain, $P_{\text{meas}}(t, \nu)$ is the measured power spectrum, $\eta(\nu)$ is the transmission efficiency of the antenna, and $P_{\text{short}}(\nu)$ is the measured power spectrum from the short.

We use the diurnal variation of the Galactic signal to calculate the system gain $K(\nu)$ using a χ^2 fit with equal weighting:

$$\chi^2(\nu) = \sum_t [T_{\text{meas}}(t, \nu) - T_{\text{GSM}}(t, \nu)]^2 \quad (3)$$

and minimizing with respect to $K(\nu)$. Fig. 3 shows the time dependence of $T_{\text{meas}}(t, \nu)$ at a single frequency.

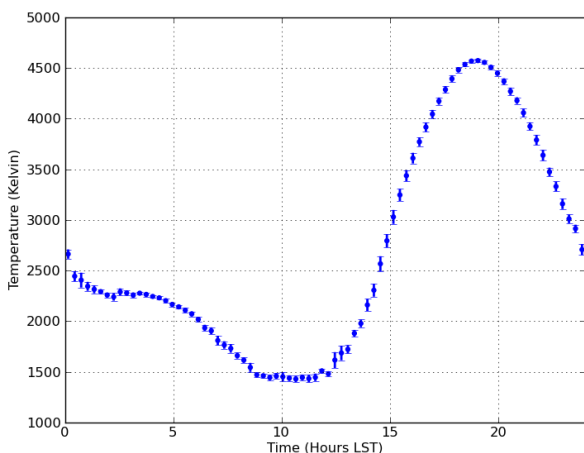


FIG. 3.— Diurnal variation of a single 2 MHz wide bin centered at 70 MHz. Calibrated mean with RMS error bars are shown for 9 days of observation binned in ~ 18 minute intervals. Variation in the errors at different times is due to varying amounts of exposure time caused by RFI excised and corrupted spectra.

Each day of data is averaged to provide a single spectrum $\langle T_{\text{meas}} \rangle_{\text{DAY}}(\nu)$. This spectrum is fit to a

model of the Galactic sky-averaged brightness temperature ($T_{\text{GM}}(\nu)$):

$$\log_{10} T_{\text{GM}}(\nu) = \sum_{k=0}^n a_k \left[\log_{10} \left(\frac{\nu}{70 \text{ MHz}} \right) \right]^k \quad (4)$$

Using the calculated a_k for each day of data, the residuals $\Delta T(\nu) = \langle T_{\text{meas}} \rangle_{\text{DAY}}(\nu) - T_{\text{GM}}(\nu)$ are calculated. These $\Delta T(\nu)$ values are our estimate of the all-sky brightness temperature spectrum after removal of Galactic emission. For $n=1$, the residuals are several Kelvin, but with $n=2$ there is significant improvement. An $n=2$ fit captures the expected foreground contributions, a power law spectral shape along with a self-absorption correction term. Adding additional a_k terms has minimal impact on the overall residual levels and we use daily $n=2$ fits for the rest of the analysis. Fig. 4 shows an example $\langle T_{\text{meas}} \rangle_{\text{DAY}}(\nu)$ spectrum with fit and residuals for a single day of observation.

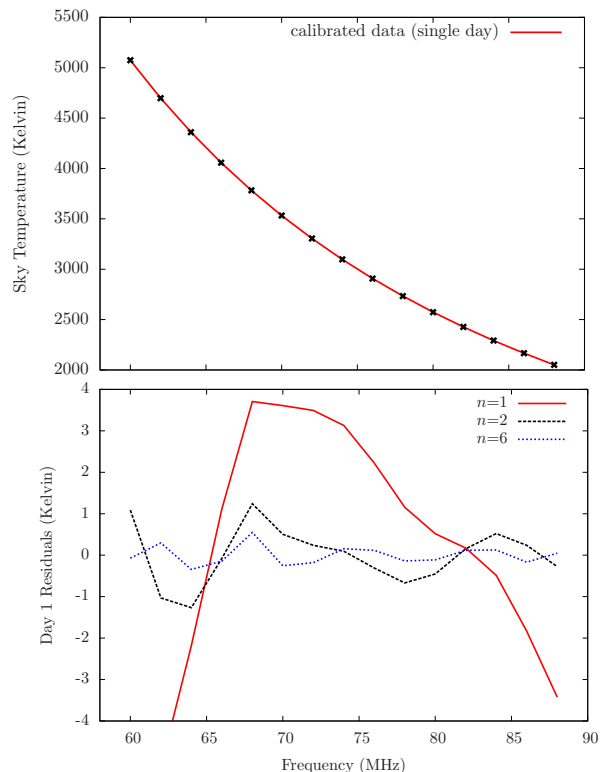


FIG. 4.— Data calibrated using the GSM (de Oliveira-Costa et al. 2008). The top plot shows mean data from a single day of observation (~ 50 minutes integration time) binned in intervals of 2 MHz. The best fit plot for $n=2$ is also shown ($a_0 = 3.548$, $a_1 = -2.360$, $a_2 = -0.164$, for June 1st). The bottom plot shows the residuals after the fit was subtracted. A simple power law ($n=1$) results in a poor fit, while $n=2$ substantially improves the fit.

Fig. 5 shows the mean and variance, weighted by exposure time, for fits performed with $n=2$. Our residuals are $\lesssim 1$ Kelvin, particularly near $\nu = 70$ MHz. Also shown are the predictions of three cosmological models, obtained using the SIMFAST code (Santos et al. 2010) (see also Mesinger et al. (2011)). The mean over the frequency range 60-90 MHz is subtracted from each model spectrum since for the measured brightness temperature the mean is removed by the fit.

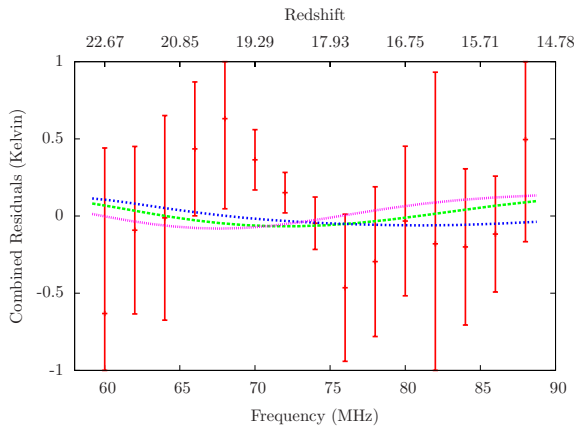


FIG. 5.— Combined residuals from 4.4 hours of integration time. The prediction of three reionization models are also plotted, differing in their star formation efficiency and X-ray heating. The mean brightness temperature is subtracted from each of the theoretical models.

4. DISCUSSION AND FUTURE WORK

Calibration, using GSM model diurnal variation, followed by a three-parameter fit to the all-sky Galactic spectrum gives residuals considerably lower than those predicted for an experiment with such a wide beam (Liu et al. 2013). This implies that the $\sim 10\%$ variance of the GSM angular structure assumed in Liu et al. (2013) is dominated by fine-scale mapping errors such as striping due to receiver gain drift as opposed to variance in the actual sky signal. With the ~ 500 mK residuals achieved, the maximum variance in Galactic angular structure is calculated at 70 MHz. This variance is equivalent to gaussian random noise with 80 Kelvin RMS amplitude, which is a factor of ten below that assumed by Liu et al. (2013) in their simulation of expected foreground structure.

Despite the wide beam of our experiment we can calibrate the all-sky brightness measurement using the diurnal variation of Galactic emission as mapped by other fine-beam observations. This is in contrast to the Bowman et al. (2008) experiment, which uses an external

noise source to calibrate the system response. The data presented here has only 4.4 hours of integration time, so thermal noise still makes a significant contribution to the residuals. Additional integration time during the galactic minimum and expansion of the frequency range should give continued improvement of the residuals, including potential detection of the 21 cm absorption trough.

The theoretical models in Fig. 5 show 300 mK peak to peak temperature amplitude. These models differ in their star formation and X-ray heating efficiencies (Santos et al. 2008), and these variations move the location and width of the minimum. To succeed in detecting such features, future data must cover a wider frequency range with higher sensitivity. In particular, it would be very useful to extend into the FM band above 87 MHz.

Planned improvements to the instrument include higher data collection efficiency and reduction of self-generated RFI in the 120 MHz frequency range. For our next observations, the team plans to travel to Isla Socorro (Latitude $18^\circ 48' 0''$ N, Longitude $110^\circ 90' 0''$ W), ~ 600 km off the Pacific coast of Mexico. This island is expected to provide an RFI environment where the FM band signals are below the thermal noise. With two full weeks of data providing over 25 hours of integration, our goal is to achieve residuals below the 100 mK level across the frequency range 40-130 MHz.

Travel to Isla Guadalupe would not have been possible without support from local agencies in Mexico, including Grupo de Ecología y Conservación de Islas A.C. (GECI), Secretaría de Marina (SEMAR), Secretaría de Gobernación (SEGOB), Comisión Nacional de Areas Naturales Protegidas (CONANP), Reserva de la Biosfera de la Isla Guadalupe, Sociedad Cooperativa de Participación Estatal Abuloneros y Langosteros, SRL., and Dr. Raúl Michel.

A.N., J.B.P., and T.C.V. acknowledge funding from NSF grant AST-1009615. A.N. thanks the McWilliams Center for Cosmology for partial financial support. JMGC and OLC thank INAOE for financial support. JMGC acknowledges a CONACyT Beca Mixta that allowed him to spend a year at the McWilliams Center for Cosmology

REFERENCES

- Abel, T., Bryan, G. L., & Norman, M. L. 2002, *Science*, 295, 93
 Bernardi, G. et al. 2013, *ApJ*, 771, 105
 Bharadwaj, S., & Ali, S. S. 2004, *MNRAS*, 352, 142
 Bowman, J. D., Rogers, A. E. E., & Hewitt, J. N. 2008, *ApJ*, 676, 1
 Bromm, V. 2013, *ArXiv e-prints*
 Bromm, V., Coppi, P. S., & Larson, R. B. 1999, *ApJ*, 527, L5
 —. 2002, *ApJ*, 564, 23
 Bromm, V., & Larson, R. B. 2004, *ARA&A*, 42, 79
 Burns, J. O. et al. 2012, *Advances in Space Research*, 49, 433
 Carilli, C. L., Furlanetto, S., Briggs, F., Jarvis, M., Rawlings, S., & Falcke, H. 2004, *New A Rev.*, 48, 1029
 Cooray, A. 2004, *Phys. Rev. D*, 70, 063509
 de Oliveira-Costa, A., Tegmark, M., Gaensler, B. M., Jonas, J., Landecker, T. L., & Reich, P. 2008, *MNRAS*, 388, 247
 Field, G. B. 1958, *Proceedings of the IRE*, 46, 240
 Furlanetto, S. R., & Briggs, F. H. 2004, *New A Rev.*, 48, 1039
 Furlanetto, S. R., Oh, S. P., & Briggs, F. H. 2006, *Phys. Rep.*, 433, 181
 Hydrogen Epoch of Reionization Array (HERA). 2010, <http://reionization.org/RFI2.HERA.pdf>
 Large-Aperture Experiment to detect the Dark Ages (LEDA). 2013, <http://www.cfa.harvard.edu/LEDA/science.html>
 Liu, A., Pritchard, J. R., Tegmark, M., & Loeb, A. 2013, *Phys. Rev. D*, 87, 043002
 Loeb, A., & Zaldarriaga, M. 2004, *Physical Review Letters*, 92, 211301
 McKee, C. F., & Tan, J. C. 2008, *ApJ*, 681, 771
 Mesinger, A., Furlanetto, S., & Cen, R. 2011, *MNRAS*, 411, 955
 Omukai, K., & Palla, F. 2001, *ApJ*, 561, L55
 —. 2003, *ApJ*, 589, 677
 Paciga, G. et al. 2011, *MNRAS*, 413, 1174
 Parsons, A. R. et al. 2013, *ArXiv e-prints*
 Pober, J. C. et al. 2013, *ApJ*, 768, L36
 Pritchard, J. R., & Loeb, A. 2010, *Phys. Rev. D*, 82, 023006
 —. 2012, *Reports on Progress in Physics*, 75, 086901
 Santos, M. G., Amblard, A., Pritchard, J., Trac, H., Cen, R., & Cooray, A. 2008, *ApJ*, 689, 1
 Santos, M. G., Ferramacho, L., Silva, M. B., Amblard, A., & Cooray, A. 2010, *MNRAS*, 406, 2421
 Square Kilometer Array (SKA). 2013, <http://www.skatelescope.org/>
 Tan, J. C., & McKee, C. F. 2004, *ApJ*, 603, 383
 van Haarlem, M. P. et al. 2013, *A&A*, 556, A2
 Wouthuysen, S. A. 1952, *AJ*, 57, 31